NIWA

Taihoro Nukurangi

Spatial distribution of the burrows of scampi, *Metanephrops challengeri*, and implications for the design of photographic abundance surveys

Tim Watson
Martin Cryer

Final Research Report for
Ministry of Fisheries Research Projects
SCI2001/01 (Objective 3)

National Institute of Water and Atmospheric Research

May 2003

Final Research Report

1.	**Date:**	31 May 2003
2.	**Contractor:**	National Institute of Water & Atmospheric Research Ltd
3.	**Project Title:**	"Measuring the abundance of scampi"
4.	**Project Codes:**	SCI 2001/01
5.	**Project Leader:**	Martin Cryer
6.	**Duration of Project:**	
	Start date:	1 December 2000
	Expected completion date:	31 March 2003

7. Executive Summary:

The spatial distribution of burrows thought to have been built by scampi was examined using counts from digital photographs taken in 2000, 2001, and 2002 surveys in the Bay of Plenty. The statistical distribution of these counts was significantly different from random (Poisson) and was best simulated using a negative binomial distribution with low–moderate patchiness. However, in a subset (drawn from all surveys) of transects containing many photographs, there was no significant autocorrelation between counts from adjacent photographs at scales of 10–100 m. A more comprehensive analysis of spatial contagion using variograms suggested that this result was true throughout the core area of the QMA 1 scampi fishery at scales of 10–1000 m. We conclude that there is more variation among counts than would be expected in a random field, but the source of this variation is not simple contagion (animals clustering together). Based on these inferences, we established a model population and used it to test the performance of alternative sampling strategies for photographic surveys of scampi burrows. When the number of photographs at a station was held constant, we observed the usual pattern of a decreasing CV with increasing number of stations in the survey. We also observed the usual pattern of a decreasing CV with increasing sample size (i.e., the number of photographs taken) at each station. However, when deployment time, steaming between stations, and burrow counting were included as "costs" the pattern became complex. In all cases, the optimum number of transects within a station was one. Incorporating multiple transects at a station, initially implemented to facilitate comparison between trawl and photographic methods of estimating relative abundance, is inefficient and should be discontinued unless comparison of trawl and photographic estimates is a priority. Ignoring counting time and spatial structure suggested that the optimal strategy would be to maximise the number of images collected within a given time constraint, and this led to a survey design with very few stations each with a very large numbers of images. This is not logistically possible given current technology, and would produce survey results sensitive to changes in spatial pattern and subject to occasional

imprecise estimates. More robust and feasible strategies include more stations with fewer images at each; a reasonable balance between expected precision and robustness occurs between 5 and 12 stations per stratum with 40–10, respectively, photographs at each.

8. Objectives:

Overall Objective for both projects:

1. To estimate the abundance of scampi (*Metanephrops challengeri*).

Relevant Objectives for SCI2001/01:

3. To examine the effects of spatial distribution of scampi on the precision and bias of estimates of abundance derived from photographic surveys, and make recommendations on any future changes to the design of the survey techniques.

9. Methods:

9.1 Analysis of spatial distribution of scampi burrows

9.1.1 Data

Stratified random photographic surveys of scampi burrows within the core area of the QMA 1 scampi fishery (Cuvier Island to White Island, 300–500 m depth) were undertaken in 1998, 2000, 2001, and 2002 (Cryer et al., 2002, Figure 1). In 1998, a *Benthos* emulsion based system was used. In 2000 and subsequent years a custom built system using digital cameras was used. Only data from the digital system are used for this study because the locations of stations were not recorded with sufficient precision in 1998.

9.1.2 Field sampling

Each survey 2000–2002 consisted of about 20 stations, each station 2 or 3 (usually 3) transects, and each transect of (nominally) 12–15 photographs. Within a station, transects were spaced about 1000 m apart at roughly constant depth, such that each station mimicked a short trawl tow (the original intent of this design was to compare photographic and trawl methods of sampling scampi). Within a transect, photographs were taken as the ship drifted, using a time delay sufficient to ensure that adjacent photographs did not overlap (Cryer & Hartill 1998, Cryer et al., 2001). Image sizes were determined using parallel lasers.

9.1.3 Estimating the density of scampi burrows

Each image considered to be sufficiently clear and unobstructed was "initiated" (Cryer et al., 2002), and its readable area defined. Each of three readers then assessed the number of burrow openings using the standardized protocol described by Cryer et al.,

For this study, we used the average of the three counts of major burrow openings (see Figure 2 for an example) divided by the readable area as a density estimator for each image. Other indices could be used, including the density of visible scampi, the density of all burrow openings, or the density of minor openings, but we think that the density of major openings is the best index of scampi abundance because it should be unaffected by changes in emergence behaviour or burrow structure.

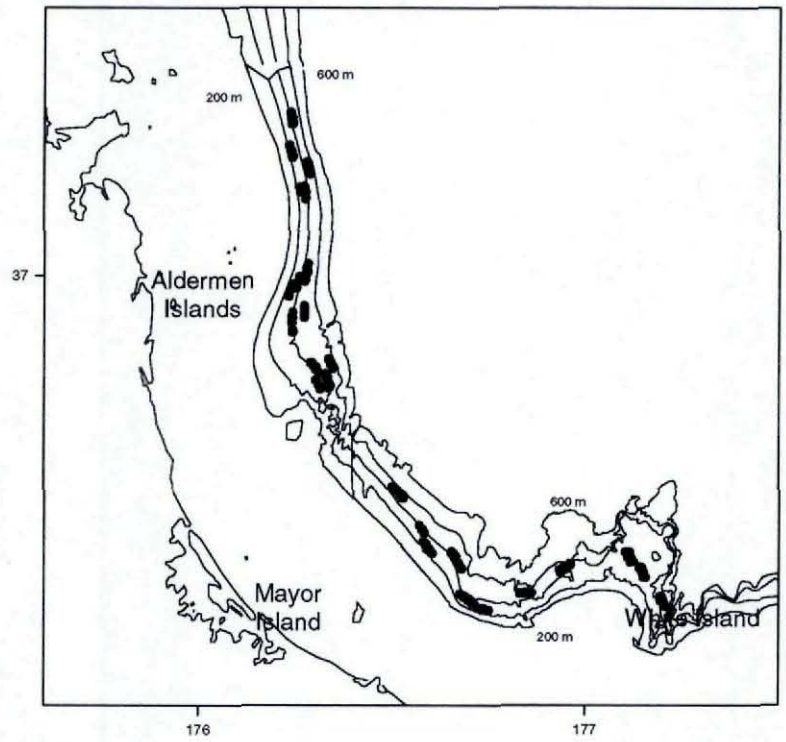

***Figure 1*: Sampling strata for photographic surveys of scampi and scampi burrows in the "core" area of the QMA 1 fishery, 1998–2002) and distribution of images used in this study (dots). Generally, each station consisted of three transects about 1000 m apart, and each transect consisted of 10–20 images spaced 5–40 m apart. Isobaths are shown at 100 m intervals from 200 to 600 m.**

***Figure 2*: New Zealand scampi, *Metanephrops challengeri*, emerging from a highly characteristic "major" burrow opening.**

9.1.4 Analysis of spatial pattern

When considering the "patchiness" of scampi burrows, we applied two approaches; the first was concerned only with the statistical distribution of density, whereas the second was concerned with the location as well as statistical distribution. The difference between the two approaches can best be visualised by considering a population of random numbers sorted along some geographical (or other) gradient; treatment of the numbers as independent would detect no deviation from a random distribution, and detecting the association with the gradient requires that the position on the gradient is known too.

9.1.4.1 Overdispersion of counts

If animals (or their burrows) are distributed at random within an area (one of our strata, for instance), then the statistical distribution of density will conform to a Poisson distribution:

$$p_x = \frac{e^{-\lambda}\lambda^x}{x!}$$

where p_x is the probability of exactly x burrow openings being counted in an image and λ is the overall average number of burrow openings per image. If burrows are "contagiously" distributed in some way (because some areas are better habitat than others, or because scampi naturally aggregate into patches), then the Poisson distribution will generate too low a probability for zero and high counts. In this event, the counts are said to be "overdispersed", the distribution of burrows is non-normal in me way, and the Poisson distribution is inappropriate as a model. Overdispersed counts can be modelled using a negative binomial distribution, which can be parameterised as:

$$p_x = \frac{\Gamma(x+k)}{x!\Gamma(k)}\left(\frac{\lambda}{k+\lambda}\right)^x\left(\frac{1}{1+\frac{\lambda}{k}}\right)^k \qquad \text{var} = \lambda + \frac{\lambda^2}{k}$$

where p_x is the probability of exactly x burrow openings being counted in an image, λ is the overall average number of burrow openings per image, and k is the overdispersion parameter. It can be shown that as k gets large the negative binomial approaches the Poisson model.

9.1.4.2 Autocorrelation of counts

A simple method of including both the size and position of a datum into an analysis is to correlate each count with its nearest neighbour, so called autocorrelation. Given

measurements, Y_1, Y_2, ..., Y_n at locations X_1, X_2, ..., X_n (assumed to be equally spaced), the lag-q autocorrelation function is defined as:

$$r_q = \frac{\sum_{i=1}^{n-q}(Y_i - \bar{Y})(Y_{i+q} - \bar{Y})}{\sum_{i=1}^{n}(Y_i - \bar{Y})^2}$$

which is a correlation coefficient with n-2 degrees of freedom. However, instead of correlation between two different variables, autocorrelation measures the association for the same variable at locations (or times) X_i and X_{i+q}. When the autocorrelation is used to detect non-randomness, it is usually only the first (q=1) autocorrelation that is of interest, although it is frequently plotted for many lags when exploring spatial pattern in detail.

9.1.4.3 Variograms

The data were transferred into GeoR (1) for spatial analysis. GeoR provides functions for geostatistical data analysis using the statistical software R. Of particular interest is the production of empirical variograms. Variograms provide a measure of the strength of the variance and correlation between samples at varying distances (and optionally the direction). Typically, all possible sample pairs are examined and grouped into classes (lags) of approximately equal distance and direction. A Variogram provides a means of quantifying the commonly observed relationship that samples close together will tend to have more similar values than samples far apart. The classical estimate of the variogram formula is:

$$2\gamma(h) = \frac{1}{N_{ij}} \sum_{i=1}^{n} \sum_{j<i} \left[Z(s_i) - Z(s_j) \right]^2$$

where $Z(s_i)$ and $Z(s_j)$ are sampled points in the random field Z(s), N_{ij} the number of sampled points, h the difference over all points, $2\gamma(h)$ the variogram function and $\gamma(h)$ the semi-variogram. Variograms were computed in GeoR using the *variog()* function, summarised in Table 1 with the main arguments. Omnidirectional variograms were constructed over the whole geographic range after converting the coordinate system to metric units. Each sampling point (the location of each image) was considered as an individual and independent location representing the mean density.. The nugget tolerance was set to 7 m (similar to the minimum distance between images); pairs of points closer together than 7 m were considered co-located and not considered for estimating variogram. The variograms were binned and smoothed over a variety of distances to assess spatial pattern on a variety of scales.

9.2 Modelling sampling strategies for photographic surveys

The objective of the sampling model analysis was to optimize the number of stations, the number of transects, and the number of images within each transect so as to

minimize the coefficient of variance (c.v.) of the estimate of overall mean density. In this instance, the c.v. is defined as:

$$cv = \frac{s}{\sqrt{n}} \Big/ \mu$$

where s is the sample standard deviation, μ the sample mean, and n the number of stations.

***Table 1*: Implementation of variogram model:** variog geodata, uvec = "default", ..., option = c("bin", "cloud", "smooth") ,..., nugget.tolerance = 0, max.dist, ..., direction = "omnidirectional",...) **in the GeoR statistical package.**

Argument	Details
Geodata	a list containing element coords as described next. Typically an object of the class "geodata" - a geoR data-set. If not provided the arguments coords must be provided instead.
Cords	an n x 2 matrix containing coordinates of the n data locations in each row. Defaults to geodata$cords, if provided.
Data	a vector or matrix with data values. If a matrix is provided, each column is regarded as one variable or realization. Defaults to geodata$data, if provided.
Uvec	a vector with values defining the variogram binning. Only used when option = "bin". See DETAILS below for more details on how to speficy the bins.
Option	defines the output type: the options "bin" returns values of binned variogram, "cloud" returns the variogram cloud and "smooth" returns the kernel smoothed variogram. Defaults to "bin".
nugget.tolerance	a numeric value. Points which are separated by a distance less than this value are considered co-located. Defaults to zero.
max.dist	a numerical value defining the maximum distance for the variogram. Pairs of locations separated for distance larger than this value are ignored for the variogram calculation. If not provided defaults takes the maximum distance among all pairs of data locations.
Direction	a numerical value for the directional (azimuth) angle. This used to specify directional variograms. Default defines the omnidirectional variogram. The value must be in the interval [0, pi] radians ([0, 180] degrees).

We first constrained the analysis to a single stratum having a fixed sampling time of one (12 h) ship day. The stratum was assumed to be long and narrow (as are the real strata in QMAs 1 and 2) and was approximated by a one dimensional grid of length 70 km, split into 5000 intervals of 14 m each. For each simulation, station(s) were located randomly within the stratum and burrow counts were generated at the necessary number of adjacent grid points by selecting at random from a negative binomial distribution with an "overdispersion parameter" k = 6.25. This was estimated using the estimated sample mean (0.75 burrows per image) and its estimated variance (0.84):

$$\text{var} = \lambda + \frac{\lambda^2}{k}$$

where k is the overdispersion parameter and λ is the mean. Each strategy was simulated 100 times and the average of the estimated c.v. calculated. The sampling time "costs" of each strategy (Table 2) were also calculated. Simulations were done to find the optimal number of images per station that minimizes the c.v. between stations. Again, each strategy was optimized over 100 simulations and the mean c.v. calculated.

Table 2: **Time cost categories and their methods of calculation.**

Description	Method of calculation	Value
Total sampling time	Fixed	12 hours
Steaming between stations	Calculated using ship speed (18k.h^{-1}) and the generated total distance between stations	Random each simulation
Steaming between transects	Calculated using ship speed (18k.h^{-1}) and distance between transects (1 km)	3.24 minutes
Drifting between images	Fixed	1 minute
Camera deployment	20 minutes down and 20 minutes up	40 minutes per transect

10. Results

10.1 Spatial distribution of scampi burrows

10.1.1 General patterns

Although we have not conducted an exhaustive analysis of variance, there were no apparent geographical differences or trends in the mean density of scampi burrows or in its variability (Figure 3); all areas from the Aldermen Islands to White Island exhibited a range of estimated densities from zero to ~0.8 m^{-2}. This wide variation in the estimated density of scampi burrows at the image level is not surprising because an average image of about 7 m^2 represents a small sample relative the average density of ~0.1 m^{-2}.

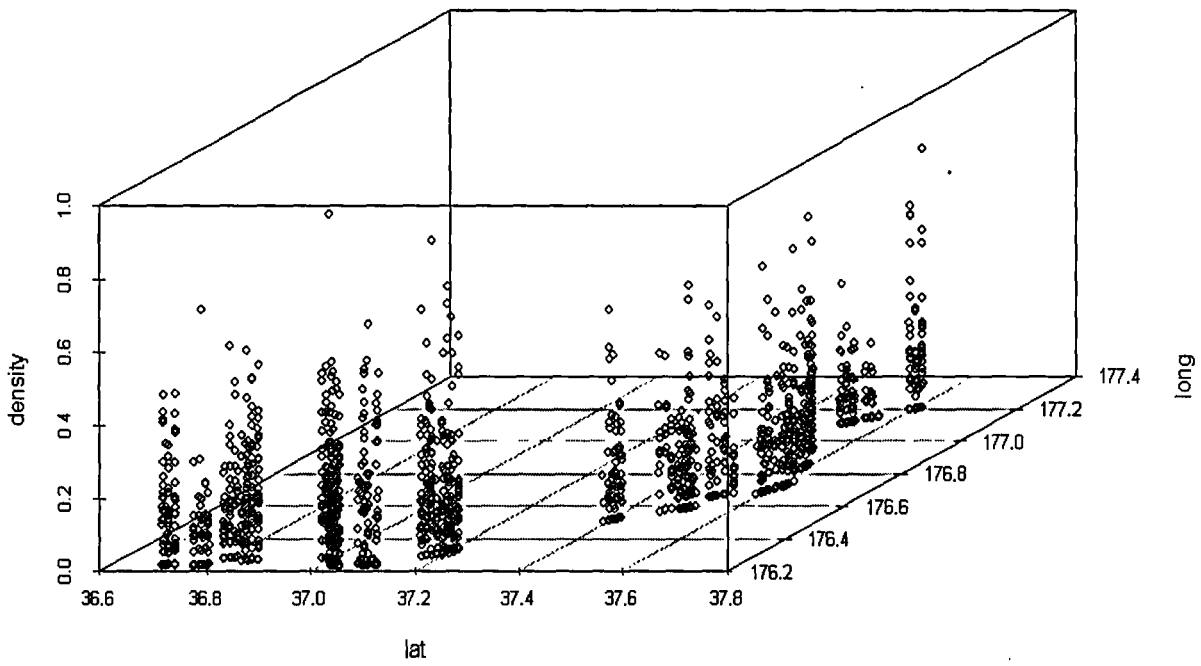

Figure 3: **Geographical distribution of estimates of density in an image.**

Some zero counts were recorded throughout the depth range 300–500 m (Figure 4), even though this is the "core" of the QMA 1 scampi trawl fishery. However, consistent with previous studies using commercial CPUE and research trawling (Cryer et al 1998, 1999) there appeared to be a broad peak in density at about 400 m depth in QMA 1.

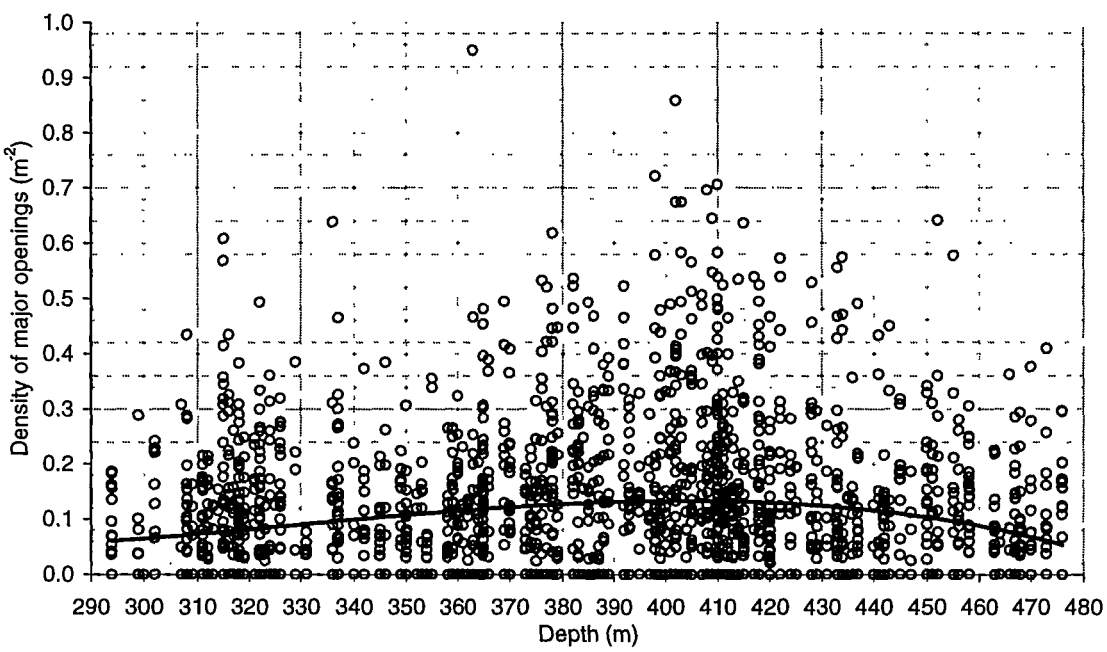

Figure 4: **Distribution of estimates of density in an image with depth. The line is a third order polynomial fitted using ordinary least squares methods, and is indicative only.**

10.1.2 Overdispersion of counts

The Poisson (random) model of counts in an image had fewer zeros and fewer high counts (4 or more) than the raw data, and slightly more counts of one (Figure 5, chi-squared "goodness of fit test, $\chi^2_6 = 15.1$, $p \sim 0.02$). A negative binomial model with a "k" parameter of 6.25 fitted the observed distribution much more closely ($\chi^2_6 = 1.8$, $p \sim 0.93$). This indicates a statistical distribution of counts that is statistically different from random, but not markedly so.

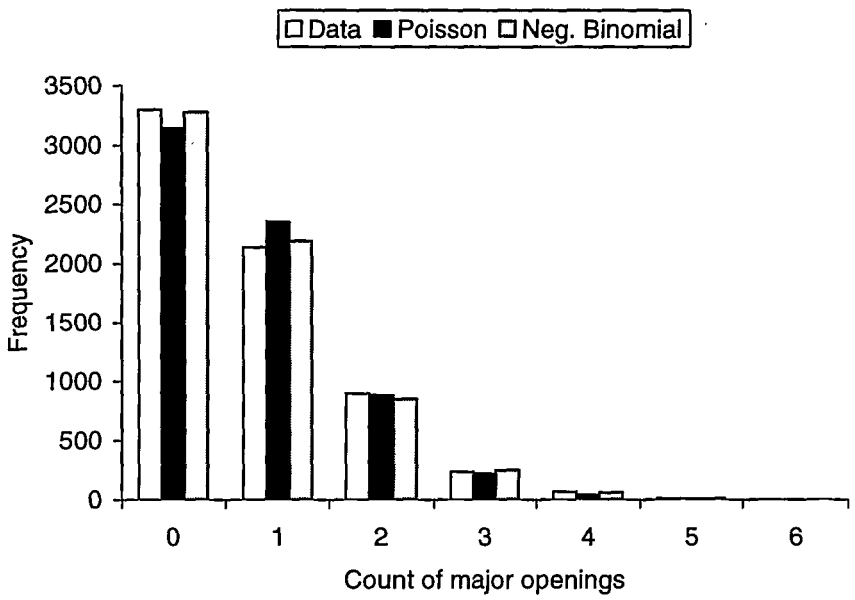

***Figure 5*: Frequency distributions of counts of major burrow openings in an image. Open bars show observed data, black and grey bars indicate Poisson (random) and best-fitting negative binomial models.**

10.1.3 Spatial pattern and autocorrelation

Based on the eight "image rich" stations we examined (five from QMA 1 covering all the years 1998 – 2002, and three from QMA 3), there was no evidence of spatial autocorrelation in the density of scampi burrows (Figure 6). This applied when comparing estimates from adjacent images (lag = q = 1), or with any greater spatial lag ($q \leq 10$). We found this a little surprising because previous work by Cryer & Hartill (1999) suggested that autocorrelation was present up to scales of a few tens of metres. However, Cryer & Hartill (1999) used an approximate method of estimating the distance between pairs of images (based on the time stamp of each image and an assumed average rate of drift) and a counting protocol developed for the burrows of *Nephrops norvegicus*. In reality, the rate of drift varied considerably throughout the 1998 survey, and no other data were recorded to enable more accurate estimates of location to be made. Also, we have since developed a more rigorous counting protocol for the burrows of *Metanephrops challengeri* which results in lower counts (though not consistently so). Thus, we consider Cryer & Hartill's (1999) examination of spatial autocorrelation to be suspect, although it is possible that the analyses presented here cannot be "extrapolated" to the higher burrow densities observed in 1998.

Similarly, our variograms do not show a general pattern of increasing variance with increasing distance between photographs at any of the spatial scales we studied from

10 to 1000 m (Figures 7 and 8). These analyses cover the whole spectrum of possible scales that we can study using photographs of ~10 m^2. Autocorrelation at a finer scale would not be relevant to our sampling problem (because it would be acting at a scale less than the separation of individual images), and autocorrelation at a larger scale would be operating at a "whole stratum" or depth band level where we would expect counts to be relatively homogeneous.

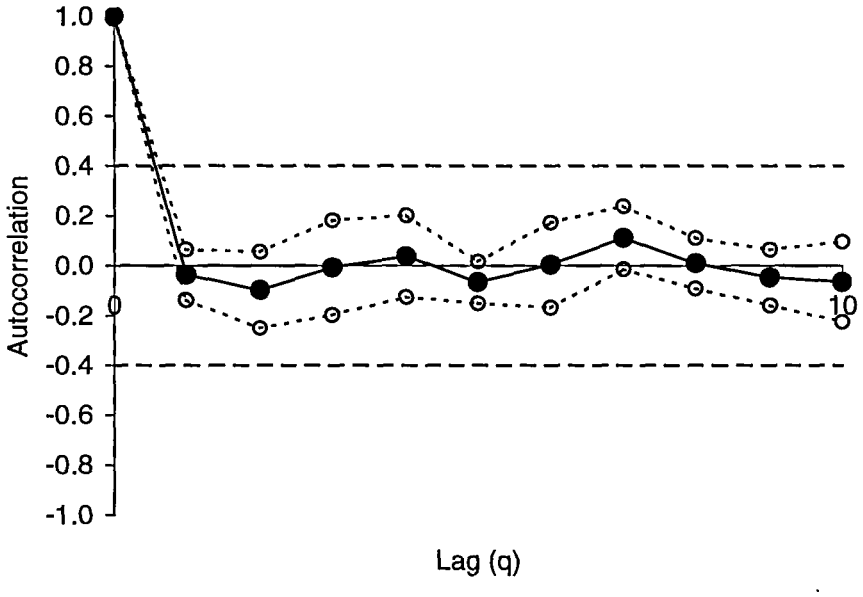

Figure 6: **Estimated mean autocorrelation coefficients (for eight transects of 35 or more images selected from surveys in QMAs 1 and 3, 1998 to 2002) with increasing spatial lag. Dotted lines indicate plus or minus one standard deviation for the mean autocorrelation, and dashed lines show approximate critical values for the correlation coefficient (α = 0.05). None of the eight transects had "significant" autocorrelation at any of the lags tested.**

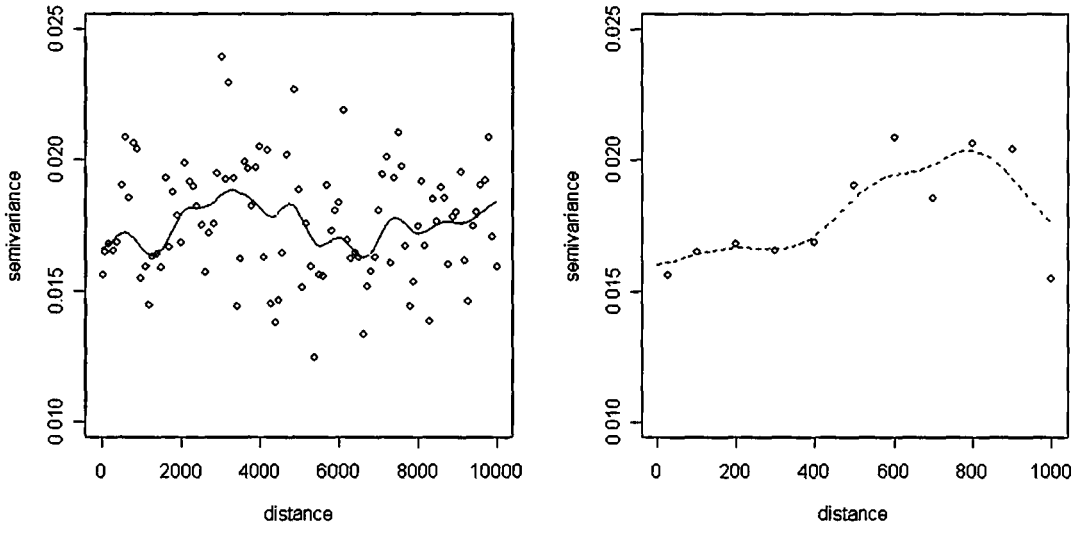

Figure 7. **Variograms – maximum distance of 10,000 m with 100 m bin widths (left) – maximum distance of 1000 m with 100 m bin widths (right). Lines are Loess smoothers.**

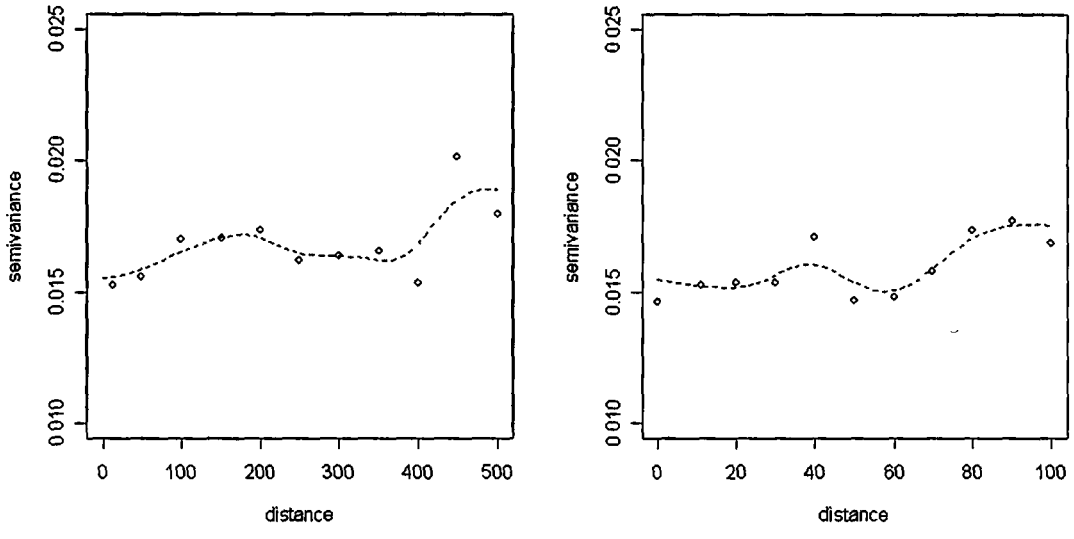

Figure 8. **Variograms – maximum distance of 500 m with 50 m bin widths (left) – maximum distance of 100 m with 10 m bin widths (right). Lines are Loess smoothers.**

10.2 Modelling sampling strategies for photographic surveys

Preliminary work suggested that, if it was no longer considered important for photographic surveys to "mimic" trawl surveys, then the number of photographic transects at each station should always be one. The mean density of burrows at each station is calculated using the number of images and their aggregate area. It follows that the reliability of the estimate of density at each station should increase as the number of images increases. The time taken to deploy and retrieve the camera for a transect (~40 minutes) is very large compared with the time between images (~1 minute). For a given amount of time (and excluding for the moment any technological constraints), therefore, the number of images will decrease sharply as the number of transects increases. This suggests there is a large "cost" of adding even a second transect at each station, and we investigated only "single transect" strategies further.

In the absence of time and cost constraints, and if the number of images at a station is fixed, the c.v. of the final estimate of abundance declines steadily as the number of stations increases (Figure 9). In models with no geographical pattern (i.e., a single "homogeneous" stratum with only sampling variability), the final c.v. also decreases steadily as the number of images at each station is increased because the estimates of density at each station become progressively closer together (each becomes, in effect, a bigger sample). Both results are to be expected from standard sampling theory.

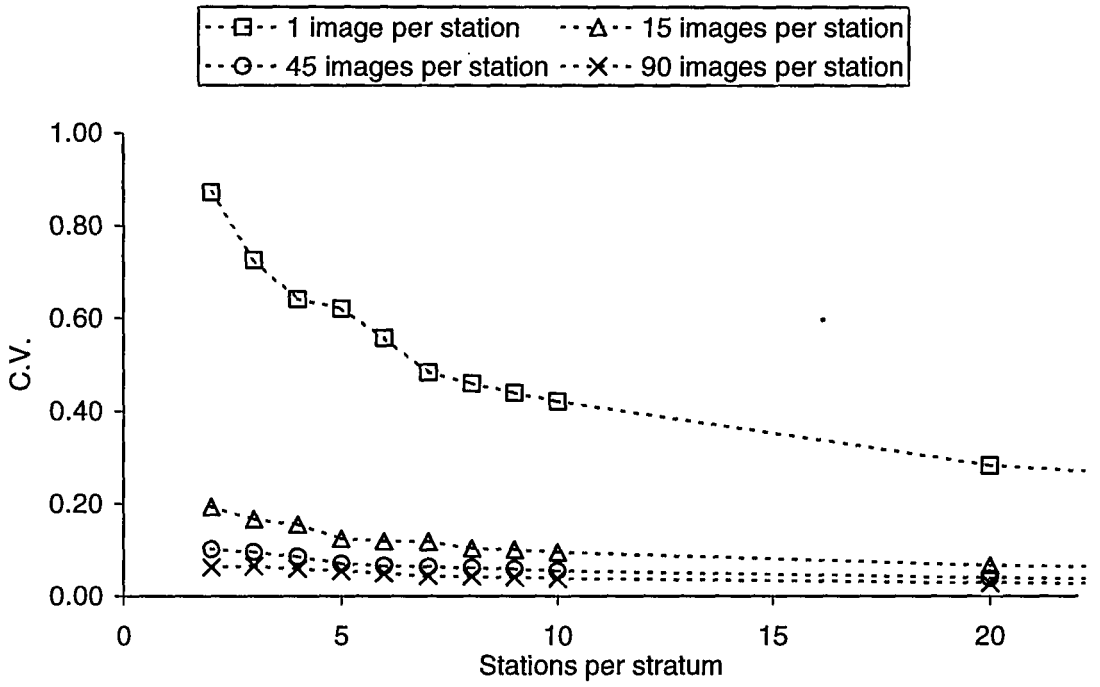

Figure 9. **Relations among number of stations, number of images at each, and the C.V. of the estimate of overall density for strategies with fixed allocations of images per station.**

If sampling is constrained to a 12 hour day and the number of images at a station is optimized (for that number of stations), then the c.v. increases steadily as the number of stations increases (Figure 10); the two-station strategy is optimal. This might be considered counter-intuitive, but is analogous to the problem of multiple transects at a station; deploying and retrieving the camera for a station and steaming between stations takes a long time compared with taking more photographs.

Unfortunately, the two-station approach requires about 300 photographs to be taken at each station (i.e., 600 in total). This has a high analytical cost (each photograph is screened by three people and then discussed) estimated to be approximately $15 per image. In addition, we have not imposed any large-scale variation in density in the stratum and have assumed it to be homogenous (though with overdispersion of counts at an ill-defined scale). Our analysis broadly supports this assumption, but any geographical pattern would tend to favour strategies with many stations over those with few.

Another important consideration in the strategy chosen is the risk of image loss; weather, sea conditions, or equipment failure can result in some or all images from a deployment not being useful. By increasing the number of stations we enable more opportunity of adaptation and feedback during a survey. For example, if a five-station strategy was implemented and the camera were to fail for some reason on one whole station, then the remaining stations could probably be modified to compensate. Conversely, a camera failure within a two-station strategy would result, proportionally, in a very large loss of data that could not be reasonably compensated by modifying the other station in that stratum. Thus, although a two-station model appears optimal in terms of minimizing the stratum c.v. for a given amount of ship time, it has major disadvantages in terms of the number of photographs needing

screening, its lack of robustness to changes in distribution and patchiness, and the risk of time loss following camera or image failure.

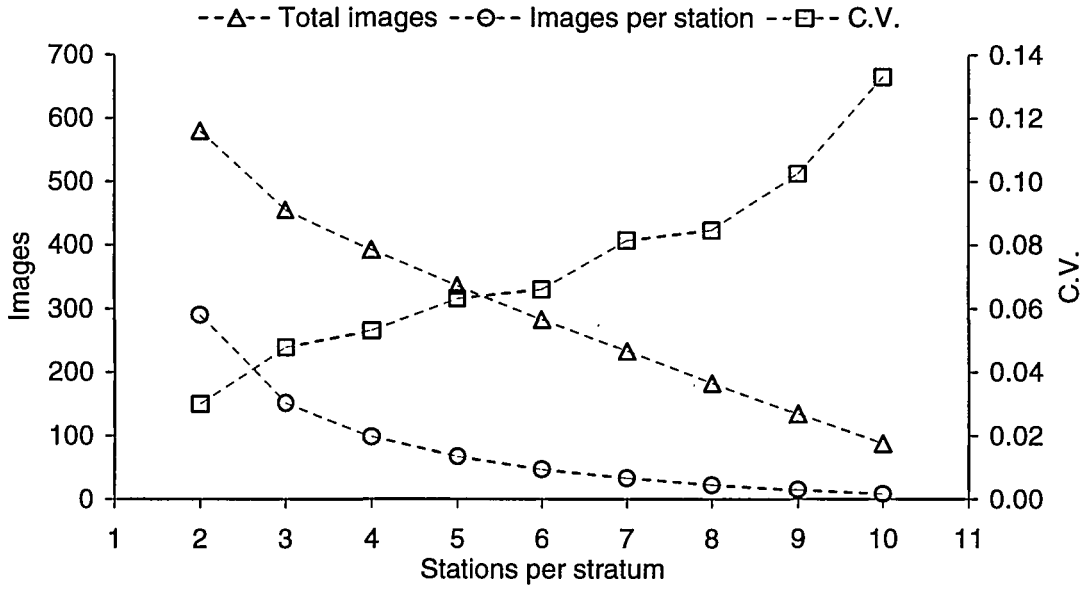

Figure 10. **Relations among the number of stations, the number of images possible at each when ship time is constrained, and the mean predicted survey C.V. for photographic strategies of 2–10 stations per stratum.**

Incorporating counting costs as well as ship time costs essentially completes the optimization; all other costs (project set up, steaming to and from the sampling area from the vessel's home port, data analysis, reporting, etc) are, for all practical purposes, fixed. When the overall cost of estimating the average density of burrows within a stratum is constrained (to, for example $15 000), a tradeoff between the costs of ship time and counting becomes apparent (Figure 11). For set numbers of stations from 2 to 20, we searched for an allocation of images to each station that minimized the expected estimated c.v. for the given cost. The number of images per station affects both ship time and counting costs, but acts more directly on the latter. Each strategy was simulated 100 times, using different random stations each time, and the average expected C.V. and its maximum were estimated. The maximum observed C.V. from these simulations was adopted as an indicator of the least precise result likely using a particular strategy.

For a given total cost, a sampling strategy with just two stations per stratum (and lots of photographs at each) still gives the lowest expected C.V.. The expected average C.V. increases with increasing numbers of stations per stratum, but does not increase rapidly until more than about 8–10 stations per stratum are considered (Figure 11). The risk of generating an imprecise result is quite high for strategies with very few or very many stations, but is lower for strategies with about 5–12 stations per stratum. Taken together, these results suggest that strategies with about 5–12 stations per stratum (with 40–10 photographs, respectively, per station) will generate precise and robust estimates of burrow density with little risk of an imprecise result and good ability for in-survey compensation for technical problems. The balance between ship time and counting time changes markedly across this range, but the overall results are quite similar. Outside this range, however, the results become sensitive to, or reliant

on, a very few stations or on the interpretation of a relatively small numbers of photographs.

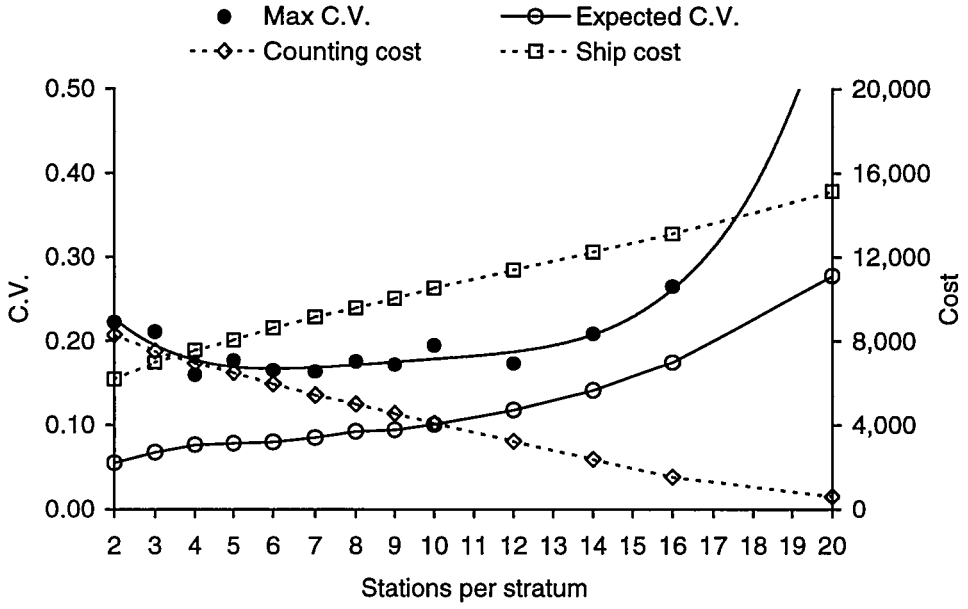

***Figure 11*: Relations among costs, mean predicted survey C.V., and the maximum likely C.V. (from 100 simulations) for photographic strategies of 2–20 stations per stratum where the total cost was constrained. The line fitted to the Maximum C.V. data points is a fourth-order polynomial and is indicative only.**

11. Conclusions:

1. Scampi burrows are not distributed randomly within the core area of the QMA 1 scampi trawl fishery (Mercury Islands to White Island, 300–500 m depth). There is a weak relationship with depth (peak density at about 410 m), but no obvious large-scale geographical pattern.

2. Counts of scampi burrows are mildly overdispersed ("patchy") and the data are better represented by a negative binomial distribution than by a Poisson distribution.

3. Over scales of 10–1000 m, autocorrelation analysis of stations with a lot of data and variogram analysis of the whole data set revealed no strong and consistent spatial pattern.

4. Based on these findings we built an operating model of a population of scampi burrows consisting of a one-dimensional stratum with point estimates of density at intervals of about 14 m, similar to the typical spacing of images in current surveys. Point estimates were selected from a negative binomial distribution, but no overall spatial structure was imposed. We sampled the model using a variety of sampling strategies.

5. Sampling the operating model using our current design of five stations with about 40 photographs at each generated estimates of average density with better precision (lower CVs) than we observe in the field. This suggests that there is more variability among real stations than there is in our relatively simple model.

6. If resources were unlimited, surveys with more stations per stratum produce more precise results and surveys with more images per station produce more precise results. Both are to be expected from standard sampling theory.

7. There is no advantage in using more than one transect per station unless there are technical constraints imposed by the number of images that need to be collected at a station.

8. If ship time is constrained, surveys with two stations per stratum and very large numbers of images per station produce the most precise results. The counting costs associated with such a design would be very high, however.

9. If a constraint is place on total cost (ship time plus counting time, with no constraint on the balance between the two), surveys with two stations per stratum still produce the most precise results on average. However, surveys with few stations sometimes produced imprecise results and have some substantial operational and technical limitations.

10. When the total cost is constrained, surveys of 5–12 stations per stratum (20–48 stations in total) produce robust estimates of the mean density of burrows and its variance with little loss of precision compared with the theoretical optimal survey.

References cited:

Annala, J.H.; Sulllivan, K.J.; O'Brien, C.J. (2000). Report from the Fishery Assessment Plenary, May 2000: stock assessments and yield estimates. 495 p. (Unpublished report held in NIWA library, Wellington.)

Cryer, M. (2002). Voyage Report for voyage KAH0203, Project SCI2001/01, R.V. *Kaharoa*, Bay of Plenty, April 2002. (Unpublished report held by Ministry of Fisheries, Wellington.)

Cryer, M.; Coburn, R. (2000). Scampi stock assessment for 1999. Fisheries Assessment Report 2000/07. 60 p.

Cryer, M.; Hartill, B. (1998). An experimental comparison of trawl and photographic methods of estimating the biomass of scampi. Final Research Report for Project SCI9701. 26 p. (Unpublished report held in NIWA library, Wellington.)

Cryer, M.; Hartill, B.; Drury, J. (2001). Photographic estimation of the abundance and biomass of scampi, *Metanephrops challengeri*. Final Research Report for Project SCI1999/02. 49 p. (Unpublished report held in NIWA library, Wellington.)

Hartill, B.; Cryer, M. (2002). Unstandardised scampi CPUE indices update for QMA 1 and QMA 2 including the first 6 months of the 2001–02 fishing year. Final Research Report for Project MOF2001/03R Objective 1. 16 p. (Unpublished report held in NIWA library, Wellington.)

MAF Fisheries (1990). RAND_STN v.1.7 implementation for PC computers. Software held at NIWA, Greta Pt. & Auckland offices.

Marrs, S.J.; Atkinson, R.J.A.; Smith, C.J. (1998). The towed underwater TV technique for use in stock assessment of *Nephrops norvegicus*. p 88–98 In: I.C.E.S. Report of the study group on the life histories of *Nephrops norvegicus*, La Coruña, Spain. May 1998. 155 p.

Snedecor G.W.; Cochran W.C. (1989). Statistical Methods. 8th ed. Iowa State University Press, Ames, Iowa, USA.

Tuck, I.D.; Atkinson, R.J.A.; Chapman, C.J. (1994): The structure and seasonal variability in the spatial distribution of *Nephrops norvegicus* burrows. *Ophelia* 40: 13–25.

Tuck, I.D.; Chapman, C.J.; Atkinson, R.J.A.; Bailey, N.; Smith, R.S.M. (1997). A comparison of methods for stock assessment of the Norway lobster, *Nephrops norvegicus*, in the Firth of Clyde. *Fisheries Research* 32: 89–100.

Vignaux, M. (1994). Documentation of Trawlsurvey Analysis Program. MAF Fisheries Greta Pt. Internal Report No. 225. 44 p. (Unpublished report held at NIWA library, Wellington.)

12. Publications:

There are no other publications for this objective. A Voyage Programme and a Voyage Report were submitted for *Kaharoa* voyage KAH0201, and Final Research Reports have been submitted for Objectives 1 and 2.

13. Data Storage:

Data from trawl and photographic stations are in the Empress database *trawl*. Original and annotated photographic images are held as lightly compressed JPEG files on a secure, backed-up server and in three additional copies on CD-ROM at two different sites. Copies have also been provided for the Ministry's Data Manager at Greta Point. Image details and records of readings are centralised in a formal MS-Access database on a secure, backed-up server at NIWA Auckland. Various analytical files in MS-Excel and presentations in MS-PowerPoint reside on the same server. These will be copied to the Ministry's Data Manager at Greta Point on completion of the projects.